Nonlinear Pose Tracking Controller for Bar Tethered to Two Aerial Vehicles with Bounded Linear and Angular Accelerations

Pedro O. Pereira and Dimos V. Dimarogonas

***Abstract*— We consider a system composed of a bar tethered to two aerial vehicles, and develop a controller for pose tracking of the bar, i.e., a controller for position and attitude tracking. Our first control step is to provide an input and a state transformations which convert the system vector field into one that highlights the cascaded structure of the problem. We then design a controller for the transformed system by exploring that cascaded structure. There are three main contributions: *i)* we provide bounds on the linear and angular acceleration of the bar that guarantee well-posedness of the controller, and such bounds can be used when selecting the gains and saturations of bounded controllers for both three dimensional and unit vector double integrators; *ii)* the proposed control law includes a degree of freedom which can be used to regulate the relative position between the aerial vehicles; and *iii)* the proposed control law for the throttle guarantees that the cascaded structure of the problem is preserved. Simulations are presented which validate the proposed algorithm.**

I. Introduction

Aerial vehicles provide a platform for automating inspection and maintenance of infrastructures [1]. Vertical take off and landing rotorcrafts, with hover capabilities, and in particular quadrotors, form a class of underactuated vehicles whose popularity stems from their ability to be used in small spaces, their reduced mechanical complexity, and inexpensive components [2], [3].

Slung load transportation by aerial vehicles is an important task in the scope of inspection and maintenance of infrastructures [4]. To be specific, the system we focus on is composed of a one dimensional bar and two quadrotors attached to that bar by cables. Different slung load systems and control strategies have been studied and proposed. Load lifting of a point mass by a single or multiple aerial vehicles has been studied, with focus on exploring differential flatness for the purposes of control and motion planning [5]–[8], on nonlinear control techniques for an extended range of operation [9]–[13], and on adaptive control laws for compensating model uncertainties and disturbances [14]–[16]. Experimental results are also found, with vision being used for measuring the position of the load so as to estimate the cable length [17], and with information exchange between the aerial vehicles being considered [18]. Load lifting of a rigid body by multiple aerial vehicles is also found in [19]–[21]. In [20], [21] a controller for three of more vehicles transporting a rigid body is proposed, where the throttle control laws are designed by minimizing the error to the desired 3D force requested to each vehicle. In this work, however, the proposed throttle control laws are designed so as to preserve the cascaded structure of the problem. A critical issue in trajectory tracking controllers for VTOL vehicles is the need of a bounded control law for a 3D double integrator, which guarantees well-posedness of the control law over the whole state space [3], [22]–[24]. One of our contributions is in realizing that the quadrotors-bar system is an extended VTOL vehicle, in the sense that, in addition to a bounded control law for a 3D double integrator, a bounded control law for a unit vector double integrator is also necessary.

In this manuscript, we design a control law that guarantees that the lifted bar asymptotically tracks a desired pose trajectory. The design process follows two steps: in the first, we compute an input and a state transformations, which convert the quadrotors-bar vector field into one where the cascaded structure of the problem becomes explicit; and in the second step, we explore that cascaded structure and design a controller via a backstepping procedure. There are three main contributions, which we emphasize here. First, we provide bounds on the linear and angular acceleration of the bar that guarantee well-posedness of the controller, where these bounds are necessary when selecting the gains and saturations of bounded controllers for three dimensional double integrators and unit vector double integrators. Secondly, the proposed control law includes a degree of freedom which can be used to regulate the relative position between the aerial vehicles, namely to drive the vehicles further or closer together. Finally, another novelty is that the proposed control law for the throttle guarantees the preservation of the cascaded structure of the problem.

II. Notation

The map $\mathcal{S} : \mathbb{R}^3 \ni x \mapsto \mathcal{S}(x) \in \mathbb{R}^{3\times 3}$ yields a skew-symmetric matrix and it satisfies $\mathcal{S}(a)\, b := a \times b$, for any $a, b \in \mathbb{R}^3$. $\mathbb{S}^2 := \{x \in \mathbb{R}^3 : x^T x = 1\}$ denotes the set of unit vectors in $\mathbb{R}^3$. The map $\Pi : \mathbb{S}^2 \ni x \mapsto \Pi(x) := I_3 - xx^T \in \mathbb{R}^{3\times 3}$ yields a matrix that represents the orthogonal projection onto the subspace perpendicular to $x \in \mathbb{S}^2$. We denote $A_1 \oplus \cdots \oplus A_n$ as the block diagonal matrix with block diagonal entries A_1 to A_n (square matrices). We denote by $e_1, \cdots, e_n \in \mathbb{R}^n$ the canonical basis vectors in $\mathbb{R}^n$. For some set A, id_A denotes the identity map on that set. Given some normed spaces A and B, and a function $f : A \ni a \mapsto f(a) \in B$, $Df : A \ni a \mapsto Df(a) \in \mathcal{L}(A, B)$ denotes the derivative of f. Given a manifold A, $T_a A$ denotes the tangent set of A at some $a \in A$. In [25], the reader finds all the details and proofs, some of which we omit in this manuscript due to space constraints.

The authors are with the School of Electrical Engineering, KTH Royal Institute of Technology, SE-100 44, Stockholm, Sweden. Email addresses: {ppereira, dimos}@kth.se. This work was supported by the EU H2020 Research and Innovation Programme under GA No.644128 (AEROWORKS), the Swedish Research Council (VR), the Swedish Foundation for Strategic Research (SSF) and the KAW Foundation.

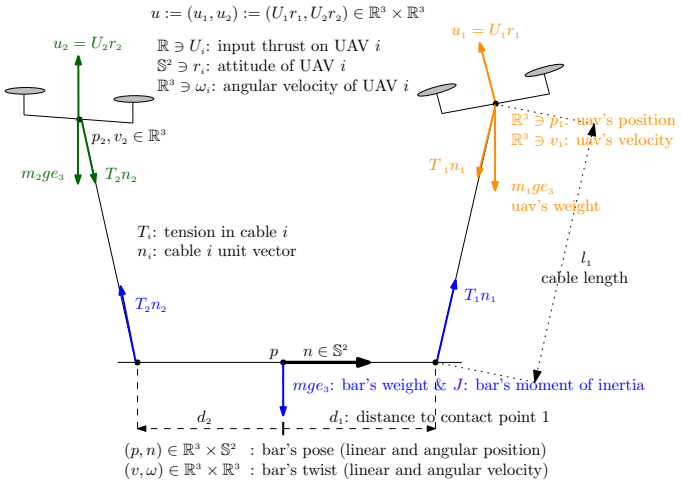

Fig. 1. Modeling of the quadrotors-bar system

III. Modeling and Problem Statement

Consider the system illustrated in Fig. 1, with two quadrotors, a one dimensional bar and two cables connecting the quadrotors to distinct contact points on the bar. All the physical quantities are those in Fig. 1. Hereafter, we refer to this system as quadrotors-bar system. As a first modeling step, we assume that we have control over the quadrotors' throttle and attitude – $u_1, u_2 \in \mathbb{R}^3$ in Fig. 1. Later, in Section VI, we let the quadrotors' attitude (i.e., $r_1, r_2 \in \mathbb{S}^2$) be part of the state, and we assume we have control over the quadrotors throttles and angular velocities (i.e., $U_1, U_2 \in \mathbb{R}$ and $\omega_{r_1}, \omega_{r_2} \in \mathbb{R}^3$). Consider then the state space in (1), which encapsulates the constraints illustrated in Fig. 1. We emphasize that the constraints in (1)-(2) imply that the distance between each contact point on the bar and the corresponding quadrotor is constant and equal to the corresponding cable length. We always decompose a $z \in \mathbb{Z}$ and a $u \in \mathbb{R}^6$ in the same way, namely $u \in \mathbb{R}^6 :\Leftrightarrow (u_1, u_2) \in \mathbb{R}^3 \times \mathbb{R}^3$ and

$$z \in \mathbb{Z} :\Leftrightarrow (z_k, z_d) \in \mathbb{Z} :\Leftrightarrow (p, n, p_1, p_2, v, \omega, v_1, v_2) \in \mathbb{Z}, \quad (4)$$

where $z_k := (p, n, p_1, p_2) \in \mathbb{Z}_k$ corresponds to the pose of the bar and positions of the vehicles (with $\mathbb{Z}_k$ as in (2)); and $z_d := (v, \omega, v_1, v_2)$ corresponds to the twist of the bar and velocities of the vehicles. The state space definition in (1) allows for the definition of the cables' unit vectors. Specifically, for $i \in \{1, 2\}$, we define

$$\mathbb{Z}_k \ni z_k \mapsto n_i(z_k) := \frac{p_i - (p + d_i n)}{\|p_i - (p + d_i n)\|} \overset{(2)}{=} \frac{p_i - (p + d_i n)}{l_i} \in \mathbb{S}^2, \quad (5)$$

where (5) can be visualized in Fig 1. Given an appropriate $u : \mathbb{R}_{\geq 0} \mapsto \mathbb{R}^6$, a system's quadrotors-bar trajectory $z : \mathbb{R}_{\geq 0} \ni t \mapsto z(t) \in \mathbb{Z}$ evolves according to

$$\dot{z}(t) = Z(z(t), u(t)), z(0) \in \mathbb{Z},$$

where $Z : \mathbb{Z} \times \mathbb{R}^6 \ni (z, u) \mapsto Z(z, u) \in \mathbb{R}^{24}$ is given by

$$Z(z, u) := \begin{bmatrix} Z_k(z_k) z_d \\ Z_d(z, u) \end{bmatrix} \left(= \begin{bmatrix} \dot{z}_k \\ \dot{z}_d \end{bmatrix} \right) \in \mathbb{R}^{24}, \quad (6)$$

where

$$Z_k(z_k) := (I_3 \oplus -\mathcal{S}(n) \oplus I_3 \oplus I_3) \in \mathbb{R}^{12 \times 12},$$

$$Z_d(z, u) := \begin{bmatrix} \sum \frac{T_i(z,u)}{m} n_i(z_k) - g e_3 \\ \sum \frac{T_i(z,u)}{J} \mathcal{S}(d_i n) n_i(z_k) \\ \frac{u_1}{m_1} - \frac{T_1(z,u)}{m_1} n_1(z_k) - g e_3 \\ \frac{u_2}{m_2} - \frac{T_2(z,u)}{m_2} n_2(z_k) - g e_3 \end{bmatrix} \left(= \begin{bmatrix} \dot{v} \\ \dot{\omega} \\ \dot{v}_1 \\ \dot{v}_2 \end{bmatrix} \right),$$

with g as the acceleration due to gravity; and T_1, T_2 as the tensions on the cables (see Fig 1). The linear and angular accelerations in (6) are written from the Newton-Euler's equations of motion, considering the net force and torque on each rigid body: the bar is taken as a rigid body (with net force and torque in blue – see Fig. 1); while the quadrotors are taken as point masses (with net forces in orange and green – see Fig. 1). The tensions T_1 and T_2 constitute internal forces to the quadrotors-bar system, and the Newton-Euler's equations of motion do not provide any insight into these forces. However, the constraint that the state trajectory must remain in the state set $\mathbb{Z}$ in (1), enforces the vector field Z in (6) to be in the tangent set of $\mathbb{Z}$, i.e., in $T_{z \in \mathbb{Z}} \mathbb{Z}$ (this set is here omitted for brevity). This constraint uniquely defines the tensions on the cable, i.e., for any $(z, u) \in \mathbb{Z} \times \mathbb{R}^6$, $Z(z, u) \in T_z \mathbb{Z} \Rightarrow (T_1(z, u), T_2(z, u))$ as in (3). We can now formulate the problem treated in this paper.

Problem 1: Given the vector field Z in (6) and a desired bar pose, i.e., $(p^\star, n^\star) : \mathbb{R}_{\geq 0} \ni t \mapsto (p^\star(t), n^\star(t)) \in \mathbb{R}^3 \times \mathbb{S}^2$, design a control law $u^{cl} : \mathbb{R}_{\geq 0} \times \mathbb{Z} \mapsto \mathbb{R}^6$ such that $\lim_{t \to \infty} (p(t) - p^\star(t), n(t) - n^\star(t)) = 0_6$ along a solution $\mathbb{R}_{\geq 0} \ni t \mapsto z(t) \in \mathbb{Z}$ of $\dot{z}(t) = Z(z(t), u^{cl}(t, z(t)))$.

We emphasize that the vector field (6) is input affine: to be specific, $Z(z, u) = A(z) + \begin{bmatrix} 0_{12 \times 6}^T & B(z_k)^T \end{bmatrix}^T u$, for some $A(z) \in \mathbb{R}^{24}$ and $B(z_k) \in \mathbb{R}^{12 \times 6}$ that are be found in [25].

IV. Control Law Design

Let us explain the pursued control strategy, which is illustrated in Fig. 2. As a first step, we introduce an input transformation from $\nu := (T_1, T_2, \tau_1, \tau_2) \in \mathbb{R}^8$ to $u \in \mathbb{R}^6$, where T_i and τ_i will stand for the tension and angular acceleration of cable $i \in \{1, 2\}$. As shall be seen later, ν provides a more meaningful input to design, and once it is

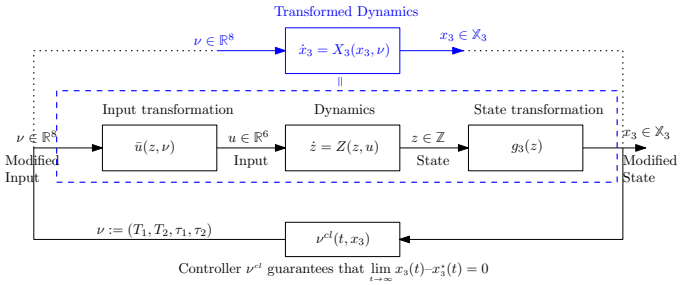

Fig. 2. Control strategy: we provide an input and state transformations which convert the vector field Z into the vector field X_3 which, in turn, highlights the cascaded structure of the problem.

$$\mathbb{Z} = \left\{ (p, n, p_1, p_2, v, \omega, v_1, v_2) \in (\mathbb{R}^3)^8 : (p, n, p_1, p_2) \in \mathbb{Z}_k, n^T \omega = 0, (v_i - (v + d_i \mathcal{S}(\omega) n))^T (p_i - (p + d_i n)) = 0, i \in \{1, 2\} \right\}, \quad (1)$$

$$\mathbb{Z}_k = \left\{ (p, n, p_1, p_2) \in \times (\mathbb{R}^3)^4 : n^T n = 1, (p_i - (p + d_i n))^T (p_i - (p + d_i n)) = l_i^2, i \in \{1, 2\} \right\}. \quad (2)$$

$$\begin{bmatrix} T_1(z, u) \\ T_2(z, u) \end{bmatrix} = \begin{bmatrix} 1 + \frac{m}{m_1} + \frac{m d_1^2}{J} \|a\|^2 & c + \frac{m d_1 d_2}{J} a^T b \\ c + \frac{m d_1 d_2}{J} a^T b & 1 + \frac{m}{m_2} + \frac{m d_2^2}{J} \|b\|^2 \end{bmatrix}^{-1} \left(\begin{bmatrix} \frac{m n_1(z_k)^T u_1}{m_1} \\ \frac{m n_2(z_k)^T u_2}{m_2} \end{bmatrix} + m \begin{bmatrix} \frac{\|v_1 - (v + d_1 \mathcal{S}(\omega) n)\|^2}{l_1} \\ \frac{\|v_2 - (v + d_2 \mathcal{S}(\omega) n)\|^2}{l_2} \end{bmatrix} + m \|\omega\|^2 \begin{bmatrix} d_1 n^T n_1(z_k) \\ d_2 n^T n_2(z_k) \end{bmatrix} \right) \overset{\substack{c = n_1(z_k)^T n_2(z_k) \\ a = \mathcal{S}(n) n_1(z_k) \\ b = \mathcal{S}(n) n_2(z_k)}}{=: M_T(z_k) u + \begin{bmatrix} T_1(z, 0_6) \\ T_2(z, 0_6) \end{bmatrix}}. \quad (3)$$

designed one can map ν to u (the actual input) by means of the function $\bar{u}$ (see Fig. 2). This is done in Section IV-B

In the second step, done in Section IV-C, we provide a coordinate transformation g_3 that maps a $z \in \mathbb{Z}$ into an $x_3 \in \mathbb{X}_3$ (g_3 and $\mathbb{X}_3$ are defined later), and with this coordinate transformation, we obtain a new vector field X_3, which comes from the composition of the vector field Z with the input transformation and the coordinate change. The benefit of this coordinate transformation is that it highlights the cascaded structure of the problem, namely the cascaded nature of X_3.

From the desired pose trajectory in Problem 1, one can compute a corresponding desired trajectory in X_3, i.e., $x_3^\star : \mathbb{R}_{\geq 0} \to X_3$. In the final step, done in Section V, and by exploiting the cascaded nature of X_3, one designs a control law

$$\mathbb{R}_{\geq 0} \times \mathbb{X}_3 \ni (t, x_3) \mapsto \nu^{cl}(t, x_3) \in \mathbb{R}^8 \tag{7}$$

that guarantees that $\lim_{t\to\infty} x_3(t) - x_3^\star(t) = 0$. By means of the mapping $\bar{u}$ (see Fig. 2), a control law in the original system may constructed, i.e.,

$$\mathbb{R}_{\geq 0} \times \mathbb{Z} \ni (t, z) \mapsto u^{cl}(t, z) := \bar{u}(z, \nu^{cl}(t, x_3))|_{x_3 = g_3^{-1}(\bar{z})}, \tag{8}$$

which then guarantees that Problem 1 is accomplished.

A. Angular velocity and acceleration of cables

In order to construct the input and coordinate transformation, illustrated in Fig. 2, we must define the angular velocity and acceleration of the cables. Consider then a smooth function $f : \mathbb{Z}_k \ni z_k \mapsto f(z_k) \in \mathbb{R}^3$ where f has constant norm pointwise (i.e., $\|f(z_k)\| = d_f$ for some $d_f > 0$ and for all $z_k \in \mathbb{Z}_k$). We can then define

$$\begin{aligned} &n_f : \mathbb{Z}_k \ni z_k \mapsto n_f(z_k) := \tfrac{f(z_k)}{d_f} \in \mathbb{S}^2, \\ &\omega_f : \mathbb{Z} \ni (z_k, z_d) \mapsto \omega_f(z_k, z_d) (= \mathcal{S}(n_f)\, \dot{n}_f) \in \mathbb{R}^3, \\ &\tau_f : \mathbb{Z} \times \mathbb{R}^6 \ni (z, u) \mapsto \tau_f(z, u) (= \dot{\omega}_f) \in \mathbb{R}^3, \end{aligned} \tag{9}$$

where n_f is the unit vector associated to f, ω_f is the angular velocity of n_f, and τ_f is the angular acceleration of n_f, along the vector field in (6). Because the vector field is input affine, the angular acceleration in (9) can be expressed as

$$\tau_f(z, u) = A_{n_f}(z) + B_{n_f}(z_k) u. \tag{10}$$

for some $A_{n_f}(z) \in \mathbb{R}^3$ $B_{n_f}(z_k) \in \mathbb{R}^{3\times 6}$ (found in [25]). For our purposes, we are interested in the angular acceleration of the cables, thus we consider, for $i \in \{1, 2\}$, the functions

$$f_i : \mathbb{Z}_k \ni z_k \mapsto f_i(z_k) := p_i - (p + d_i n) \in \mathbb{R}^3.$$

We know from (2) that $d_{f_i} = l_i$, and therefore we can define the cable unit vector n_{f_i} (this is the same function as in (5)), its angular velocity ω_{f_i} and its torque τ_{f_i}.

B. Input Transformation

Let us now provide the input transformation $\bar{u}$ illustrated in Fig. 2. For that purpose we introduce a function

$$R : \mathbb{Z} \times \mathbb{R}^6 \ni (z, u) \mapsto R(z, u) \in \mathbb{R}^m \tag{11}$$

of $m \in \mathbb{N}$ *physical quantities* we wish to regulate/control. In particular, we wish to control 6 quantities: the two tensions on the cables (2 quantities, namely T_1 and T_2), and the angular accelerations on each cable ($2 \times 2 = 4$ quantities: note that the angular accelerations τ_{f_1} and τ_{f_2} are three dimensional, but each angular acceleration is orthogonal to the corresponding cable, which means that we only need to control $2 \times (3 - 1)$ quantities). As such, we define

$$R(z, u) := \begin{bmatrix} T_1(z, u) \\ T_2(z, u) \\ \tau_{f_1}(z, u) \\ \tau_{f_2}(z, u) \end{bmatrix} = \underbrace{\begin{bmatrix} T_1(z, 0_6) \\ T_2(z, 0_6) \\ A_{n_{f_1}}(z) \\ A_{n_{f_2}}(z) \end{bmatrix}}_{=: A_R(z) \in \mathbb{R}^8} + \underbrace{\begin{bmatrix} e_1^T M_T(z_k) \\ e_2^T M_T(z_k) \\ B_{n_{f_1}}(z_k) \\ B_{n_{f_2}}(z_k) \end{bmatrix}}_{=: B_R(z_k) \in \mathbb{R}^{8\times 6}} u, \tag{12}$$

where we made use of (3) and of (10). We note that, given any $(z, \nu) \in \mathcal{V} := \{(z, \nu) \in \mathbb{Z} \times \mathbb{R}^8 : \nu := (T_1, T_2, \tau_1, \tau_2) \in \mathbb{R}^{2+6}, \tau_1^T n_1(z) = 0, \tau_2^T n_1(z) = 0\}$ it follows that there exists a unique $\bar{u} : \mathcal{V} \ni (z, \nu) \mapsto \bar{u}(z, \nu) \in \mathbb{R}^6$ such that $\nu = R(z, \bar{u}(z, \nu))$ and it is given by

$$\bar{u}(z, \nu) := (B_R(z_k)^T B_R(z_k))^{-1} B_R(z_k)^T (\nu - A_R(z)). \tag{13}$$

Notice that there exists an inverse on (13), which depends exclusively on the kinematic configuration, and it can be shown that (13) is well defined for any $z_k \in \mathbb{Z}_k$ [25].

C. State Transformation

Let us now provide the coordinate transformation illustrated in Fig. 2, which will emphasize the cascaded structure of the problem. Due to this cascaded structure, let us make the following cascaded set definitions, namely,

$$\mathbb{X}_1 := \{x_1 := (p, v, n, \omega) \in (\mathbb{R}^3)^4 : n \in \mathbb{S}^2, \omega^T n = 0\}, \tag{14a}$$
$$\mathbb{X}_2 := \{x_2 := (x_1, n_1, n_2) \in \mathbb{X}_1 \times (\mathbb{S}^2)^2\}, \tag{14b}$$
$$\mathbb{X}_3 := \{x_3 := (x_2, \omega_1, \omega_2) \in \mathbb{X}_2 \times (\mathbb{R}^3)^2 : \omega_i^T n_i = 0\}. \tag{14c}$$

We always decompose an $x_1 \in \mathbb{X}_1$, an $x_2 \in \mathbb{X}_2$ and an $x_3 \in \mathbb{X}_3$ as decomposed in (14a)–(14c). Consider then the mappings

$$\mathbb{Z} \ni z \mapsto g_1(z) := (p, v, n, \omega) \in \mathbb{X}_1, \tag{15a}$$
$$\mathbb{Z} \ni z \mapsto g_2(z) := (g_1(z), n_{f_1}(z_k), n_{f_2}(z_k)) \in \mathbb{X}_2, \tag{15b}$$
$$\mathbb{Z} \ni z \mapsto g_3(z) := (g_2(z), \omega_{f_1}(z), \omega_{f_2}(z)) \in \mathbb{X}_3, \tag{15c}$$

where g_1 isolates the pose of the bar, and the twist of the bar; while g_2 and g_3 map also to the cables' unit vectors and the cables' angular velocities (see Section IV-A for those definitions). The inverse mapping $g_3^{-1} : X_3 \ni x_3 \mapsto g_3^{-1}(x_3) \in \mathbb{Z}$ exists but it is omitted (see [25]).

It then follows that (denote $\nu := (T_1, T_2, \tau_1, \tau_2) \in \mathbb{R}^{2+6}$)

$$\begin{aligned} X_3(x_3, \nu) &:= Dg_3(z)\mathbb{Z}(z, \bar{u}(z, \nu))|_{z = g_3^{-1}(x_3)} \in T_{x_3}\mathbb{X}_3. \\ &= \begin{bmatrix} X_2(x_2, (T_1, T_2, \omega_1, \omega_2)) \\ \Pi(n_1)\, \tau_1 \\ \Pi(n_2)\, \tau_2 \end{bmatrix} \left(= \begin{bmatrix} \dot{x}_2 \\ \dot{\omega}_1 \\ \dot{\omega}_2 \end{bmatrix} = \dot{x}_3 \right), \end{aligned} \tag{16}$$

where (denote $\nu_2 := (T_1, T_2, \omega_1, \omega_2) \in \mathbb{R}^{2+6}$)

$$X_2(x_2, \nu_2) := \begin{bmatrix} X_1(x_1, (n_1, n_2), (T_1, T_2)) \\ \mathcal{S}(\omega_1)\, n_1 \\ \mathcal{S}(\omega_2)\, n_2 \end{bmatrix} \left(= \begin{bmatrix} \dot{x}_1 \\ \dot{n}_1 \\ \dot{n}_2 \end{bmatrix} \right), \tag{17}$$

and where (denote $\nu_1 := (T_1, T_2) \in \mathbb{R}^2$)

$$X_1(x_1,(n_1,n_2),\nu_1) := \begin{bmatrix} v \\ \frac{T_1 n_1 + T_2 n_2}{m} - g e_3 \\ \mathcal{S}(\omega)\, n \\ \mathcal{S}(n)\, \frac{d_1 T_1 n_1 + d_2 T_2 n_2}{J} \end{bmatrix} \left(= \begin{bmatrix} \dot{p} \\ \dot{v} \\ \dot{n} \\ \dot{\omega} \end{bmatrix} \right). \quad (18)$$

The choice of the mappings in (15) and of $\bar{u}$ in (13) is now clear: it induces a cascaded structure with three layers in (16)–(18), which can be explored in the control design process. Recall Problem 1, and note that one can then compute the desired equilibrium in $\mathbb{X}_3$: i.e., $x_3^\star : \mathbb{R}_{\geq 0} \to \mathbb{X}_3$ can be computed where $(p^\star, n^\star)|_{x_3^\star} = (p^\star, n^\star)|_{\text{Prob. 1}}$.

V. Backstepping control

The next subsections are dedicated to each of the three layers, and for the control design, we apply a backstepping procedure, similar to the one found in [24].

A. Step 1

We focus first on the first layer, and thus on the vector field (18). Consider then the following similar vector field (denote $\mathcal{T} := (\mathcal{T}_1, \mathcal{T}_2) \in \mathbb{R}^{3+3}$)

$$\mathbb{X}_1 \times \mathbb{R}^6 \ni (x_1, \mathcal{T}) \mapsto \mathcal{X}_1(x_1, \mathcal{T}) := \begin{bmatrix} v \\ \frac{\mathcal{T}_1 + \mathcal{T}_2}{m} - g e_3 \\ \mathcal{S}(\omega)\, n \\ \mathcal{S}(n)\, \frac{d_1 \mathcal{T}_1 + d_2 \mathcal{T}_2}{J} \end{bmatrix}, \quad (19)$$

where we observe that, as long as $\mathcal{T} = (\mathcal{T}_1, \mathcal{T}_2) \in (\mathbb{R}^3 \backslash \{0_3\})^2$

$$X_1\left(x_1, \left(\tfrac{\mathcal{T}_1}{\|\mathcal{T}_1\|}, \tfrac{\mathcal{T}_2}{\|\mathcal{T}_2\|}\right), (\|\mathcal{T}_1\|, \|\mathcal{T}_2\|)\right) = \mathcal{X}_1(x_1, \mathcal{T}). \quad (20)$$

The idea in the first step is then to find a control law for $\mathcal{T} = (\mathcal{T}_1, \mathcal{T}_2)$ in (19) such that Problem 1 is accomplished. Immediately after, and based on observation (20), we define the desired cable $i \in \{1, 2\}$ direction as the unit vector given by $\mathcal{T}_i$. The critical issue, and one of our contributions, is in guaranteeing that $\mathcal{T}_i$ does not vanish, which requires a bounded controller for a 3D double integrator and a unit vector double integrator.

Given $r > 0$, denote $\mathcal{B}(r) := \{\xi \in \mathbb{R}^3 : \|\xi\| \leq r\}$. Given $\bar{a}, \bar{\tau} > 0$ and $k \in \mathbb{R}$, consider then $\mathbb{X}_1 \times \mathcal{B}(\bar{a}) \times \mathcal{B}(\bar{\tau}) \ni (x_1, a, \tau) \mapsto \bar{\mathcal{T}}^{cl}(x_1, a, \tau) := (\bar{\mathcal{T}}_1^{cl}(x_1, a, \tau), \bar{\mathcal{T}}_2^{cl}(x_1, a, \tau)) \in \mathbb{R}^6$ defined as

$$\begin{bmatrix} \bar{\mathcal{T}}_1^{cl}(x_1, a, \tau) \\ \bar{\mathcal{T}}_2^{cl}(x_1, a, \tau) \end{bmatrix} := \tfrac{1}{d_1 - d_2} \begin{bmatrix} -d_2 m I_3 & J I_3 \\ d_1 m I_3 & -J I_3 \end{bmatrix} \begin{bmatrix} a + g e_3 \\ k n - \mathcal{S}(n)\, \tau \end{bmatrix} \quad (21)$$

and, it follows that composing (19) with (21) yields

$$\mathcal{X}_1(x_1, \bar{\mathcal{T}}^{cl}(x, a, \tau)) := \begin{bmatrix} v \\ a \\ \mathcal{S}(\omega)\, n \\ \Pi(n)\, \tau \end{bmatrix} \left(= \begin{bmatrix} \dot{p} \\ \dot{v} \\ \dot{n} \\ \dot{\omega} \end{bmatrix} \right). \quad (22)$$

As such, a and τ in (21) can be understood as the acceleration and torques inputs on the bar, while k is a degree of freedom that can be explored for positioning the cables in different configurations, as illustrated in Fig 3. Importantly, if

$$\bar{a} + \frac{J}{m \min(|d_1|, |d_2|)} (\bar{\tau} + k) < g \quad (23)$$

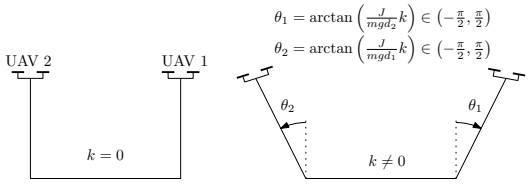

Fig. 3. Effect of degree of freedom $k \in \mathbb{R}$ in (21)

is satisfied, where $\bar{a}$ and $\bar{\tau}$ are those in the domain of (21), then neither $\bar{\mathcal{T}}_1^{cl}$ nor $\bar{\mathcal{T}}_2^{cl}$ vanish, and therefore their direction is well defined. Also, notice that the control law (21) transforms the vector field (19) into two decoupled vector fields in (22): one three dimensional double integrator related to the bar position (and controlled with $a \in \mathcal{B}(\bar{a})$), and one unit vector double integrator related with the bar attitude (and controlled with $\tau \in \mathcal{B}(\bar{\tau})$). In order to satisfy (23), the need for bounded controllers for the double integrator arises.

Remark 1: Hierarchical controllers for position trajectory tracking of VTOL vehicles require $\bar{a} < g$ for well posedness [3], [22]–[24]. The quadrotors-bar system is in essence an extended VTOL vehicle, which apart from position control also requires attitude control, giving rise to the more restrictive condition (23) for well-posedness.

Recall now Problem 1, and denote $\mathbb{P} := \mathbb{R}_{\geq 0} \times \mathbb{R}^6$ and $\mathbb{O} := \mathbb{R}_{\geq 0} \times \{(n, \omega) \in \mathbb{R}^6 : n \in \mathbb{S}^2, n^T \omega = 0\}$. Suppose then that we are given: *i)* a bounded control law law $a^{cl} : \mathbb{P} \ni (t, p, v) \mapsto a^{cl}(t, p, v) \in \mathbb{B}(\bar{a}) \subset \mathbb{R}^3$ which guarantees that $\lim_{t\to\infty}(p(t) - p^\star(t)) = 0_3$, and with a companion Lyapunov function and its non-positive derivative $\mathbb{P} \ni (t, p, v) \mapsto V_\xi(t, p, v), W_\xi(t, p, v)$; and *ii)* a bounded control law $\tau^{cl} : \Theta \ni (t, n, \omega) \mapsto \tau^{cl}(t, n, \omega) \in \mathbb{B}(\bar{\tau}) \subset \mathbb{R}^3$ which guarantees that $\lim_{t\to\infty}(n(t) \pm n^\star(t)) = 0_3$, and with a companion Lyapunov function and its non-positive derivative $\mathbb{O} \ni (t, p, v) \mapsto V_\theta(t, n, \omega), W_\theta(t, n, \omega)$. Note that the bounds on a^{cl} and τ^{cl} depend on the desired pose trajectory, so (23) imposes constraints on the desired pose trajectory: i.e., there are desired pose trajectories for which the desired cable directions may not be well defined (free falling is one example). The bounds on a^{cl} and τ^{cl} also depend on saturations and gains, which need to be chosen such that (23) is satisfied. Given the latter control laws and (21), we compose these as in

$$(t, x_1) \mapsto \mathcal{T}^{cl}(t, x_1) := \bar{\mathcal{T}}^{cl}(x_1, a^{cl}(t, p, v), \tau^{cl}(t, n, \omega)), \quad (24)$$

and, for $i \in \{1, 2\}$, we define

$$(t, x_1) \mapsto n_i^{cl}(t, x_1) := \frac{\mathcal{T}_i^{cl}(t, x_1)}{\|\mathcal{T}_i^{cl}(t, x_1)\|} \in \mathbb{S}^2, \quad (25)$$

as the desired cable i direction, and which is well defined for all $(t, x_1) \in \mathbb{R}_{\geq 0} \times \mathbb{X}_1$ provided that (23) is satisfied. Finally, notice that, given positive k_ξ and k_θ, and given

$$(t, x_1) \mapsto V_1(t, x_1) := k_\xi V_\xi(t, p, v) + k_\theta V_\theta(t, n, \omega) \geq 0, \quad (26)$$

it follows that $(t, x_1) \mapsto W_1(t, x_1) := \partial_1 V_1(t, x_1) + \partial_2 V_1(t, x_1) \mathcal{X}_1(x_1, \mathcal{T}^{cl}(t, x_1)) = k_\xi W_\xi(t, p, v) + k_\theta W_\theta(t, n, \omega) \leq 0$. We are now in position to design (T_1, T_2) as they appear in the vector field (18). Based

on (24), consider then the control law for the tensions as

$$(t, x_2) \mapsto T_i^{cl}(t, x_2) := n_i^T \mathcal{T}_i^{cl}(t, x_1) \in \mathbb{R}, i \in \{1, 2\}. \quad (27)$$

Composing (18) with (27), it follows that

$$X_1(x_1, (n_1, n_2), (T_1, T_2))|_{T_i = T_i^{cl}(t,x_2)} = \mathcal{X}_1(x_1, \mathcal{T}^{cl}(t, x_1)) + \\ + e_1(t, x_2),$$

$$e_1(t, x_2) := - \sum_{i \in \{1,2\}} \begin{bmatrix} 0_3 \\ \frac{1}{m} \Pi(n_i) \mathcal{T}_i^{cl}(t, x_1) \\ 0_3 \\ \frac{d_i}{J} \mathcal{S}(n) \Pi(n_i) \mathcal{T}_i^{cl}(t, x_1) \end{bmatrix}, \quad (28)$$

where e_1 can be understood as the error remaining after step 1 is finished.

B. Step 2 & 3

Due to space constraints, steps 2 and 3 are omitted in this manuscript (they are found in [25]). Let us summarize these steps, which are essentially two consecutive backstepping steps (similarly to as in [24]). In the 2nd step, we design the cables' angular velocities that steer the error e_1 in (28) to zero, and where the backstepping is built upon the Lyapunov function V_1 in (26). After this step, we are left with a 2nd error, and, in the third step, we design cables' angular accelerations that steer that 2nd error to zero. We only state here that, and the end of the 3rd step, one can construct a control law for the cables angular accelerations

$$\mathbb{R}_{\geq 0} \times \mathbb{X}_3 \ni (t, x_3) \mapsto \tau_i^{cl}(t, x_3) \in T_{n_i}\mathbb{S}^2, i \in \{1, 2\}, \quad (29)$$

at which point the control design is finished. Indeed, one can combine (27) and (30) to construct the control law in (7), defined as

$$\nu_3^{cl}(t, x_3) := (T_1, T_2, \tau_1, \tau_2)|_{T_i = T_i^{cl}(t,x_2), \tau_i = \tau_i^{cl}(t,x_3),} \quad (30)$$

which is itself used to define the control law in (8).

Theorem 2: Consider the vector field (6), and the control law (8), with double integrator control laws whose bounds satisfy (23). Then $\lim_{t\to\infty}(p(t) - p^\star(t)) = 0_3$ and $\lim_{t\to\infty}(n(t) \pm n^\star(t)) = 0_3$ along a solution of $\dot{z}(t) = Z(z(t), u^{cl}(t, z(t)))$ with $z(0) \in \mathbb{Z}$.
A proof is found in [25].

VI. Attitude Control

In Section III, we assumed that the quadrotrors were fully actuated, which is not the case in a real aerial vehicle. Consider then the augmented states

$$\bar{z} = (z, r_1, r_2) \in \tilde{\mathbb{Z}} \times \mathbb{S}^2 \times \mathbb{S}^2 =: \bar{\mathbb{Z}}, \quad (31)$$

$$x_4 = (x_3, r_1, r_2) \in \mathbb{X}_3 \times \mathbb{S}^2 \times \mathbb{S}^2 =: \mathbb{X}_4, \quad (32)$$

where $r_1, r_2 \in \mathbb{S}^2$ stand for the quadrotors' direction where throttle is provided (see Fig. 1); and with z as in (4) and x_3 as in (14c). The state $\bar{z} : \mathbb{R}_{\geq 0} \ni t \mapsto \bar{z}(t) \in \bar{\mathbb{Z}}$ evolves according to $\dot{\bar{z}}(t) = \bar{Z}(\bar{z}(t), u(t)), \bar{z}(0) \in \bar{\mathbb{Z}}$, where $\bar{Z} : \bar{\mathbb{Z}} \times \mathbb{R}^8 \ni (\bar{z}, u) \mapsto \bar{Z}(\bar{z}, u) \in T_{\bar{z}}\bar{\mathbb{Z}}$ is given by (denote $u := (U_1, U_2, \omega_{r_2}, \omega_{r_1}) \in \mathbb{R}^{2+6}$)

$$\bar{Z}(\bar{z}, u) := \begin{bmatrix} Z(z, (U_1 r_1, U_2 r_2)) \\ \mathcal{S}(\omega_{r_1}) r_1 \\ \mathcal{S}(\omega_{r_2}) r_2 \end{bmatrix} \left(= \begin{bmatrix} \dot{z} \\ \dot{r}_1 \\ \dot{r}_2 \end{bmatrix} \right), \quad (33)$$

with the vector field Z as in (6) (in Section III, we took $u_i = U_i r_i \in \mathbb{R}^3$ as an input, which meant we had immediate control over the vehicles' attitude, namely $r_i \in \mathbb{S}^2$ – see Fig. 1). One must now design control laws for the throttles (U_1 and U_2) and angular velocities (ω_{r_1} and ω_{r_2}) for each quadrotor. Given the control law (8), one may be tempted to choose $(t, \bar{z}) \mapsto U_i^{cl}(t, \bar{z}) := r_i^T u_i^{cl}(t, z) \in \mathbb{R}$, as it minimizes the error to the desired input, i.e., $U_i^{cl}(t, \bar{z}) = \inf_{U_i \in \mathbb{R}} \|U_i r_i - u_i^{cl}(t, z)\|$ [21]. However, if that choice is made, the cascaded structure in Section IV-C is lost.

Notice that given any $u \in \mathbb{R}^3$ and $n, r \in \mathbb{S}^2$ with $n^T r \neq 0$, the equality $\frac{n^T u}{n^T r} r = u + \frac{1}{n^T r} \mathcal{S}(n) \mathcal{S}(r) u$ holds. With that in mind, consider then $\bar{\tilde{\mathbb{Z}}} := \{\bar{z} \in \bar{\mathbb{Z}} : r_i^T n_i(z_k) > 0, i \in \{1, 2\}\}$ and the throttle control laws, for $i \in \{1, 2\}$,

$$\mathbb{R}_{\geq 0} \times \bar{\tilde{\mathbb{Z}}} \ni (t, \bar{z}) \mapsto U_i^{cl}(t, \bar{z}) := \frac{n_i(z_k)^T u_i^{cl}(t, z)}{n_i(z_k)^T r_i} \in \mathbb{R}, \quad (34)$$

and thus

$$U_i^{cl}(t, \bar{z}) r_i = u_i^{cl}(z) + \underbrace{\frac{\mathcal{S}(n_i(z_k)) \mathcal{S}(r_i) u_i^{cl}(t, z)}{r_i^T n_i(z_k)}}_{=: e_{4,i}(t, \bar{z})}, \quad (35)$$

where the error $e_{4,i}$ is orthogonal to the cable i (i.e., to n_i). Recall from (3) that the tensions depend on $n_1^T u_1$ and $n_2^T u_2$, and thus, it follows from (35) that with the choice in (34) the tensions remain unchanged, i.e., it follows from composing (12) with (35) that

$$R(z, (u_1, u_2))|_{u_i = U_i^{cl}(t,\bar{z}) r_i} = R(z, u^{cl}(t, z)) + \begin{bmatrix} 0_{2\times 6} \\ B_{n_{f_1}}(z_k) \\ B_{n_{f_2}}(z_k) \end{bmatrix} \begin{bmatrix} e_{4,1}(t, \bar{z}) \\ e_{4,2}(t, \bar{z}) \end{bmatrix}.$$

As such, for $g_4 : \bar{\mathbb{Z}} \ni \bar{z} \mapsto g_4(\bar{z}) := (g_3(z), r_1, r_2) \in \mathbb{X}_4$ and $g_4^{-1} : \mathbb{X}_4 \ni x_4 \mapsto (g_3^{-1}(x_3), r_1, r_2) \in \bar{\mathbb{Z}}$ it follows that

$$Dg_4(\bar{z}) \bar{Z}(\bar{z}, (U_1, U_2, \omega_{r_1}, \omega_{r_2}))|_{U_i = U_i^{cl}(t,\bar{z}), \bar{z} = g_4^{-1}(x_4)} \\ = \begin{bmatrix} X_3(x_3, \nu^{cl}(t, x_3)) \\ \\ 0_3 \\ 0_3 \end{bmatrix} + \left(\begin{bmatrix} \begin{bmatrix} 0_{18\times 6} \\ B_{n_{f_1}}(z_k) \\ B_{n_{f_2}}(z_k) \end{bmatrix} \begin{bmatrix} e_{4,1}(t, \bar{z}) \\ e_{4,2}(t, \bar{z}) \end{bmatrix} \\ \mathcal{S}(\omega_{r_1}) r_1 \\ \mathcal{S}(\omega_{r_2}) r_2 \end{bmatrix} \right)|_{\bar{z} = g_4^{-1}(x_4)},$$

where the cascaded structure becomes clear, and where we have now to pursue a fourth step, in addition the other three (X_3 is the vector field in (16), and ν^{cl} the control law designed at the end of step 3 in Section V-B). In this fourth step (corresponding to a third backstepping step), one designs the vehicles angular vehicles $\omega_{r_1}, \omega_{r_2}$ that steer the errors $B_{n_{f_1}}(z_k) e_{4,1}(t, \bar{z})$ and $B_{n_{f_1}}(z_k) e_{4,1}(t, \bar{z})$ to zero. All the details are found in [25].

VII. Simulations

Consider the system quadrotors-bar with parameters $m = 0.5\text{kg}$, $J = 0.04\text{kg}\,\text{m}^2$, $m_1 = 1.2\text{kg}$, $m_2 = 1.5\text{kg}$, $d_1 = 0.45\text{m}$, $d_2 = -0.55\text{m}$, $l_1 = 0.5\text{m}$ and $l_2 = 0.65\text{m}$. The desired position trajectory is $\mathbb{R}_{\geq 0} \ni t \mapsto p^\star(t) := r(\cos(\omega t), \sin(\omega t), 0) + (0, 0, 0.5) \in \mathbb{R}^3$ with $r = 2\text{m}$ and $\omega = 2\pi/15\text{s}^{-1}$, and the desired attitude trajectory is $\mathbb{R}_{\geq 0} \ni t \mapsto n^\star(t) := \frac{\mathcal{S}(e_3) p^{\star(1)}(t)}{\|\mathcal{S}(e_3) p^{\star(1)}(t)\|} \in \mathbb{S}^2$ (as such, we want the bar to be perpendicular to the tangent to the

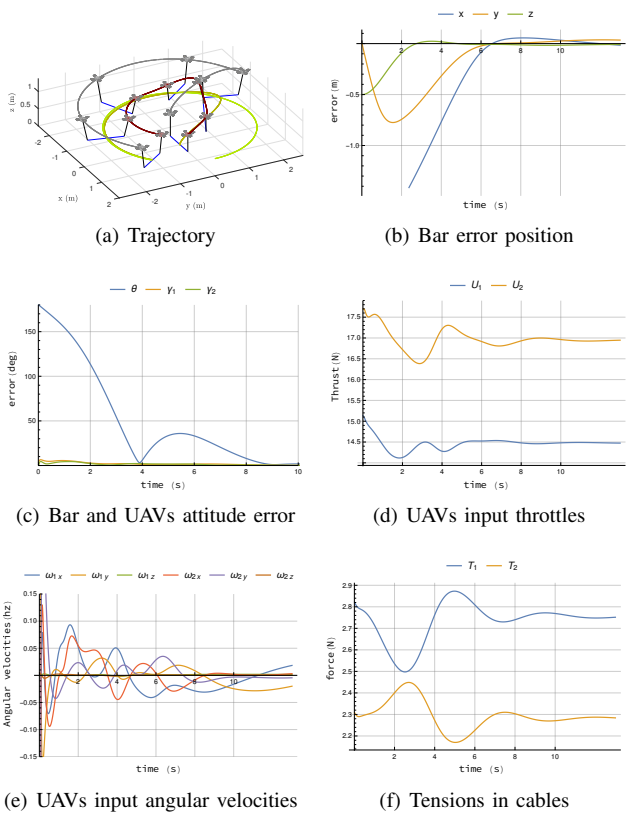

(a) Trajectory

(b) Bar error position

(c) Bar and UAVs attitude error

(d) UAVs input throttles

(e) UAVs input angular velocities

(f) Tensions in cables

Fig. 4. Trajectory for vector field (33).

path being described). The control law (8) is implemented, with $k = 0.25mgd_1/J$ (the specific controllers and their gains are found in [25]). For these choices, we provide a simulation in Fig. 4, as a solution $t \mapsto \bar{z}(t) \in \bar{\mathbb{Z}}$ of (33) composed with the proposed control law and with $\bar{z}(0) = (0_3, e_1, l_1 e_3, l_2 e_3, 0_{12}, e_3, e_3) \in \bar{Z}$. In Fig. 4(a), one can visualize the quadrotors-bar trajectory, and a visual inspection indicates position and attitude tracking. Note that, because $k > 0$, the cables are tilted away from the vertical direction, as illustrated in Fig. 3. In Figs. 4(b) and 4(c), the position and attitude errors are shown, and one verifies indeed that the error position ($t \mapsto p(t) - p^\star(t)$) and error attitude ($t \mapsto \theta(t) := \arccos(n(t)^T n^\star(t))$ are steered to zero. In Figs 4(d) and 4(e), the UAVs throttle (see (34)) and angular velocity inputs are shown. In Fig. 4(c), one verifies that the quadrotors attitude converges to the desired attitude, i.e., that $t \mapsto \gamma_i(t) := \arccos(r_i(t)^T r_i^\star(t))$ for $i \in \{1, 2\}$ is steered to zero ($r_i^\star$ is the equilibrium attitude). Finally, in Fig. 4(f) one visualizes the tensions in the cables $t \mapsto T_i(z(t), (U_1^{cl}(t, \bar{z}(t))r_1(t), U_1^{cl}(t, \bar{z}(t))r_2(t)))$ with U_i^{cl} as in (34) for $i \in \{1, 2\}$, and one verifies that those tensions are always positive, which means the cables are always taut. Deriving precise conditions on the initial state that guarantee that the tensions remain positive is a topic of future research.

REFERENCES

[1] AEROWORKS aim. http://www.aeroworks2020.eu/. Sept., 2016.

[2] R. Mahony, V. Kumar, and P. Corke. Multirotor aerial vehicles: Modeling, estimation, and control of quadrotor. *Robotics Automation Magazine, IEEE*, 19(3):20–32, Sept 2012.

[3] M. Hua, T. Hamel, P. Morin, and C. Samson. Introduction to feedback control of underactuated VTOL vehicles: A review of basic control design ideas and principles. *Control Systems*, 33(1):61–75, 2013.

[4] M. Bernard and K. Kondak. Generic slung load transportation system using small size helicopters. In *International Conference on Robotics and Automation*, pages 3258–3264. IEEE, 2009.

[5] M. E. Guerrero, D. A. Mercado, R. Lozano, and C. D. García. Passivity based control for a quadrotor UAV transporting a cable-suspended payload with minimum swing. In *2015 54th IEEE Conference on Decision and Control (CDC)*, pages 6718–6723, Dec 2015.

[6] É. Servais, H. Mounier, and B. d'Andréa Novel. Trajectory tracking of trirotor UAV with pendulum load. In *20th International Conference on Methods and Models in Automation and Robotics (MMAR)*, pages 517–522, Aug 2015.

[7] K. Sreenath, N. Michael, and V. Kumar. Trajectory generation and control of a quadrotor with a cable-suspended load - A differentially-flat hybrid system. In *International Conference on Robotics and Automation*, pages 4888–4895. IEEE, 2013.

[8] I. Palunko, R. Fierro, and P. Cruz. Trajectory generation for swing-free maneuvers of a quadrotor with suspended payload: A dynamic programming approach. In *IEEE ICRA*, pages 2691–2697, 2012.

[9] M. M. Nicotra, E. Garone, R. Naldi, and L. Marconi. Nested saturation control of an UAV carrying a suspended load. In *2014 American Control Conference*, pages 3585–3590, June 2014.

[10] T. Lee, K. Sreenath, and V. Kumar. Geometric control of cooperating multiple quadrotor UAVs with a suspended payload. In *Conference on Decision and Control*, pages 5510–5515. IEEE, 2013.

[11] K. Sreenath, T. Lee, and V. Kumar. Geometric control and differential flatness of a quadrotor UAV with a cable-suspended load. In *52nd IEEE Conference on Decision and Control*, pages 2269–2274, Dec 2013.

[12] F. A. Goodarzi, D. Lee, and T. Lee. Geometric stabilization of a quadrotor UAV with a payload connected by flexible cable. In *2014 American Control Conference*, pages 4925–4930, June 2014.

[13] É. Servais, H. Mounier, and B. d'Andréa Novel. Trajectory tracking of trirotor UAV with pendulum load. In *2015 20th International Conference on Methods and Models in Automation and Robotics (MMAR)*, pages 517–522, Aug 2015.

[14] I. Palunko, P. Cruz, and R. Fierro. Agile load transportation. *IEEE Robotics Automation Magazine*, 19(3):69–79, 9 2012.

[15] S. Dai, T. Lee, and D. S. Bernstein. Adaptive control of a quadrotor UAV transporting a cable-suspended load with unknown mass. In *Conference on Decision and Control*, pages 6149–6154. IEEE, 2014.

[16] P. Pereira, M. Herzog, and D. V. Dimarogonas. Slung load transportation with single aerial vehicle and disturbance removal. In *24th Med. Conference on Control and Automation*, pages 671–676, 2016.

[17] M. Bisgaard, A. la Cour-Harbo, and J. D. Bendtsen. Adaptive control system for autonomous helicopter slung load operations. *Control Engineering Practice*, 18(7):800–811, 2010.

[18] I. Maza, K. Kondak, M. Bernard, and A. Ollero. Multi-UAV cooperation and control for load transportation and deployment. *Journal of Intelligent and Robotic Systems*, 57(1-4):417–449, 2010.

[19] N. Michael, J. Fink, and V. Kumar. Cooperative manipulation and transportation with aerial robots. *Autonomous Robots*, 30(1):73–86, 2011.

[20] G. Wu and K. Sreenath. Geometric control of multiple quadrotors transporting a rigid-body load. In *53rd IEEE Conference on Decision and Control*, pages 6141–6148, Dec 2014.

[21] T. Lee. Geometric control of multiple quadrotor UAVs transporting a cable-suspended rigid body. In *Conference on Decision and Control*, pages 6155–6160. IEEE, 2014.

[22] D. Cabecinhas, R. Cunha, and C. Silvestre. Saturated output feedback control of a quadrotor aircraft. In *2012 American Control Conference (ACC)*, pages 4667–4602, June 2012.

[23] P. Casau, R. G. Sanfelice, R. Cunha, D. Cabecinhas, and C. Silvestre. Global trajectory tracking for a class of underactuated vehicles. In *2013 American Control Conference*, pages 419–424, June 2013.

[24] P. O. Pereira and D. V. Dimarogonas. Lyapunov-based generic controller design for thrust-propelled underactuated systems. In *2016 European Control Conference (ECC)*, pages 594–599, June 2016.

[25] P. O. Pereira and D. V. Dimarogonas. Mathematica files used in obtaining the manuscript's results. In *https://github.com/KTH-SML/nonlinear-pose-tracking-controller-for-bar-tethered-to-two-aerial-vehicles.git*.